

本文引用: 陈思睿, 吴天鸿, 刘洁, 张文青, 姚敬心, 何迎春, 史红健, 王贤文, 范婧莹. 基于网络药理学、分子对接、实验研究探讨白屈菜治疗鼻咽癌的物质基础及潜在机制[J]. 湖南中医药大学学报, 2024, 44(2): 278-287.

基于网络药理学、分子对接、实验研究探讨白屈菜治疗鼻咽癌的物质基础及潜在机制

陈思睿¹, 吴天鸿¹, 刘洁^{1,2}, 张文青^{1,2}, 姚敬心¹, 何迎春^{1,2*}, 史红健¹, 王贤文^{2,3}, 范婧莹^{1,2*}

1. 湖南中医药大学, 湖南长沙 410208; 2. 中医药防治眼耳鼻咽喉疾病湖南省重点实验室, 湖南长沙 410208;

3. 湖南中医药大学第一附属医院, 湖南长沙 410007

[摘要] **目的** 运用网络药理学和分子对接技术预测白屈菜抗鼻咽癌(nasopharyngeal carcinoma, NPC)的作用靶点和机制, 并通过实验验证主要活性成分对 NPC 细胞增殖和凋亡的影响。**方法** 借助在线数据平台 TCMSP、ETCM 和 BATMAN-TCM 检索白屈菜的化学成分和作用靶点。通过 GEO 数据库检索 NPC 相关靶点, 生信在线工具分析白屈菜与 NPC 的交集靶点。使用 STRING 构建共同靶点的 PPI 网络, 运用 Cytoscape 3.7.1 获得核心靶点。通过 R 软件编程进行 GO 功能富集分析和 KEGG 通路富集分析。分子对接分析核心靶点与主要活性成分之间的结合情况。实验验证: (1) 将 5-8F 细胞分为溶剂对照组、血根碱(2.5 $\mu\text{mol}\cdot\text{L}^{-1}$ 、5 $\mu\text{mol}\cdot\text{L}^{-1}$) 组、白屈菜红碱(2.5 $\mu\text{mol}\cdot\text{L}^{-1}$ 、5 $\mu\text{mol}\cdot\text{L}^{-1}$) 组、顺铂 4 $\mu\text{g}\cdot\text{mL}^{-1}$ 组。MTT 检测白屈菜主要活性成分对 NPC 细胞增殖的影响。(2) 将 5-8F 细胞分为溶剂对照组、血根碱 5 $\mu\text{mol}\cdot\text{L}^{-1}$ 组、白屈菜红碱 5 $\mu\text{mol}\cdot\text{L}^{-1}$ 组、顺铂 4 $\mu\text{g}\cdot\text{mL}^{-1}$ 组; Annexin-V FITC/PI 双荧光染色法检测细胞凋亡; Western blot 检测白屈菜主要活性成分对 NPC 细胞增殖、凋亡、丝裂原活化蛋白激酶(mitogen-activated protein kinase, MAPK)和磷脂酰肌醇三激酶(phosphatidylinositol 3-kinase, PI3K)/蛋白激酶 B(protein kinase B, AKT)信号通路关键蛋白的影响。**结果** 检索得到白屈菜 37 个主要活性成分和 1 419 个作用靶点。检索 GEO 数据库共收集到 7 852 个 NPC 疾病基因, 白屈菜与 NPC 共有 327 个交集靶点, 其中核心靶基因共 10 个, 分别是 EGFR、TP53、VEGFA、TNF、FN1、MMP9、JUN、FGF2、LYN、F2。GO 分析主要涉及泛素蛋白连接酶结合、硫化物结合、整合素结合、肝素结合和糖胺聚糖结合, KEGG 分析主要涉及 MAPK、PI3K/AKT 信号通路等, 分子对接结果显示核心靶点与对应的活性成分具有良好的结合能力。实验验证显示, 与溶剂对照组相比, 血根碱和白屈菜红碱均明显降低 NPC 细胞相对增殖率 ($P<0.01$), 并提高细胞凋亡率 ($P<0.01$), 且血根碱和白屈菜红碱降低 5-8F 细胞中 XIAP、PCNA、ERK1/2、AKT 的蛋白表达水平 ($P<0.05$ 或 $P<0.01$)。**结论** 白屈菜可通过多成分、多靶点和多通路发挥抗 NPC 的作用, 且经实验验证, 血根碱和白屈菜红碱均可抑制 NPC 细胞增殖并诱导凋亡, 其机制可能与 MAPK 信号通路、PI3K/AKT 信号通路有关。

[关键词] 鼻咽癌; 网络药理学; 分子对接; 白屈菜; MAPK 信号通路; PI3K/AKT 信号通路

[中图分类号] R285

[文献标志码] A

[文章编号] doi:10.3969/j.issn.1674-070X.2024.02.015

Material basis and potential mechanism of Baiqucai (Chelidonii Herba) in treating nasopharyngeal carcinoma based on network pharmacology, molecular docking, and experimental research

CHEN Sirui¹, WU Tianhong¹, LIU Jie^{1,2}, ZHANG Wenqing^{1,2}, Yao Jingxin¹, HE Yingchun^{1,2*},
SHI Hongjian¹, WANG Xianwen^{2,3}, FAN Jingying^{1,2*}

1. Hunan University of Chinese Medicine, Changsha, Hunan 410208, China; 2. Hunan Key Laboratory for Prevention &

[收稿日期] 2023-07-09

[基金项目] 国家自然科学基金资助项目(81973914); 湖南省中医药管理局项目(D2022105, B2023014); 湖南省教育厅科研项目(21C0241, 21B0358, 22C0176); 湖南中医药大学校级科研基金项目(2021XJJ014); 湖南中医药大学大学生创新课题(2022-165); 湖南中医药大学中医学一流学科开放基金项目(2021ZYX34); 长沙市自然科学基金项目(kzd22008)。

[通信作者] * 范婧莹, 女, 硕士, 讲师, E-mail: 14248623@qq.com; 何迎春, 女, 博士, 教授, 博士研究生导师, E-mail: 1305851329@qq.com。

Treatment of Ophthalmology and Otolaryngology Diseases with Chinese Medicine, Changsha, Hunan 410208, China;

3. The First Hospital of Hunan University of Chinese Medicine, Changsha, Hunan 410007, China

[Abstract] Objective To predict the action targets and mechanism of Baiqucai (*Chelidonium Herba*) against nasopharyngeal carcinoma (NPC) by network pharmacology and molecular docking techniques, and to verify the effects of its main active ingredients on the proliferation and apoptosis of NPC cells through experiments. **Methods** Through the online platforms of TCMS, ETCM, and BATMAN-TCM, the chemical constituents and action targets of Baiqucai (*Chelidonium Herba*) were searched. The relevant targets of NPC were retrieved through the GEO database, and the intersection targets of Baiqucai (*Chelidonium Herba*) and NPC were analyzed by Shengxin online tool. STRING was used to build a protein-protein interaction (PPI) network of the common targets, and Cytoscape 3.7.1 was used to obtain core targets. GO function and KEGG pathway enrichment analyses were performed by R software programming. The condition of binding between the core targets and the main active ingredients was analyzed by molecular docking. Experimental verification: (1) 5-8F cells were divided into solvent control, sanguinarine ($2.5 \mu\text{mol}\cdot\text{L}^{-1}$, $5 \mu\text{mol}\cdot\text{L}^{-1}$), chelerythrine ($2.5 \mu\text{mol}\cdot\text{L}^{-1}$, $5 \mu\text{mol}\cdot\text{L}^{-1}$), and cisplatin $4 \mu\text{g}\cdot\text{mL}^{-1}$ groups; MTT was used to test the effects of the main active ingredients of Baiqucai (*Chelidonium Herba*) on the proliferation of NPC cells. (2) 5-8F cells were divided into solvent control, sanguinarine $5 \mu\text{mol}\cdot\text{L}^{-1}$, chelerythrine $5 \mu\text{mol}\cdot\text{L}^{-1}$, and cisplatin $4 \mu\text{g}\cdot\text{mL}^{-1}$ groups; apoptosis was determined by Annexin-V FITC/PI double fluorescence staining; Western blot was used to measure the effects of the main active ingredients on the proliferation, apoptosis, as well as the key proteins of mitogen-activated protein kinase (MAPK) and phosphatidylinositol 3-kinase (PI3K)/protein kinase B (AKT) signaling pathways of NPC cells. **Results** A total of 37 main active ingredients and 1 419 action targets of Baiqucai (*Chelidonium Herba*) were obtained. A total of 7 852 NPC disease genes were collected by searching the GEO database. There were 327 intersection targets between Baiqucai (*Chelidonium Herba*) and NPC, among which ten core target genes were EGFR, TP53, VEGFA, TNF, FN1, MMP9, JUN, FGF2, LYN, and F2. GO analysis mainly involved ubiquitin protein ligase binding, ubiquitin-like protein ligase binding, sulfur compound binding, integrin binding, heparin binding, and glycosaminoglycan binding. KEGG analysis mainly involved MAPK and PI3K/AKT signaling pathways. Molecular docking showed that the core targets had good binding ability with corresponding active ingredients. The experimental verification showed that compared with the solvent control group, sanguinarine and chelerythrine significantly reduced the relative proliferation rate of NPC cells ($P<0.01$), increased the apoptosis rate ($P<0.01$), and decreased the protein expression levels of XIAP, PCNA, ERK1/2, and AKT in 5-8F cells ($P<0.05$ or $P<0.01$). **Conclusion** Baiqucai (*Chelidonium Herba*) can play an anti-NPC role through multi-component, multi-target, and multi-pathway, and it has been verified by experiments that sanguinarine and chelerythrine can both inhibit the proliferation of NPC cells and induce apoptosis, the mechanism of which may be related to MAPK and PI3K/AKT signaling pathways.

[Keywords] nasopharyngeal carcinoma; network pharmacology; molecular docking; Baiqucai (*Chelidonium Herba*); MAPK signaling pathway; PI3K/AKT signaling pathway

鼻咽癌(nasopharyngeal carcinoma, NPC)是临床常见的头颈部恶性肿瘤之一,其恶性程度高,70%的患者被确诊时已是晚期^[1-2]。以放疗和化疗相结合的综合治疗是目前治疗 NPC 的主要方法,但复发和远处转移仍是治疗失败的主要原因^[3]。目前,中医药抗肿瘤药物日益受到关注,因其与化疗药物相比,在抑杀肿瘤细胞的同时,具有毒副作用小、不易产生耐药性等优势^[4]。

白屈菜主产区位于我国东北部,是罂粟科属植物白屈菜的干燥全草,其性凉、味苦、有毒。白屈菜最早记载于《救荒本草》^[5],具有止咳平喘、消肿、利尿、

镇痛、解毒之功效。现代研究表明,白屈菜的生物活性成分在治疗癌症、呼吸道疾病、肝纤维化等方面具有研究价值^[6]。且随着人工栽培及加工技术的提高,白屈菜的产量将在未来足以提供临床药用^[7],这使其具有较高的商业前景。围绕白屈菜的抗肿瘤活性,研究发现其主要化学活性成分为异喹啉类生物碱,实验证实^[8-9],白屈菜的有效成分可通过多途径抑制肿瘤细胞增殖、促进凋亡。目前,白屈菜已用于治疗多种肿瘤,如胃癌、食管癌、肝胆肿瘤和各种中晚期肿瘤腹转移等^[10]。白屈菜的活性成分白屈菜红碱被证实非小细胞肺癌^[11]、宫颈癌^[12]等肿瘤中,都具有

较好的疗效,但在 NPC 领域尚未被广泛应用。而另一主要活性成分血根碱在 NPC 领域中的相关研究报道也较少见。目前,白屈菜治疗 NPC 的物质基础及作用机制尚不明确。

因此,本研究基于网络药理学,构建白屈菜的活性成分、NPC 与药物靶点之间的相互作用网络,借助分子对接技术分析白屈菜主要活性成分与核心靶点的结合情况,最后通过实验验证白屈菜主要活性成分对 NPC 的作用,为揭示白屈菜治疗 NPC 的物质基础及潜在分子机制提供参考。

1 材料与方 法

1.1 白屈菜作用靶点的筛选

在 TCMSp(<https://tcmsp-e.com/tcmsp.php>)、ETCM(<http://www.tcmip.cn/ETCM/>)、BATMAN-TCM 数据库(<http://bionet.ncpsb.org.cn/batman-tcm/index.php/Home/Index/index>),输入关键词“Baiqucai”“Chelidonium majus”,BATMAN-TCM 数据库选择 score>5 的靶点,合并上述结果得到白屈菜的活性成分和作用靶点,并通过 UniProt 数据中 reviewed(Swiss-Prot)and Human 矫正。

1.2 NPC 靶点的筛选

选择 GEO 数据库中与 NPC 相关的转录组数据集,分别为 GSE68799、GSE118719、GSE134884,具体信息见表 1。通过 R 语言 V 4.1.3“DEseq2”“limma”等分析 3 个转录组,选择 $P<0.05$, $|\log_2FC|>1$ 的基因为差异基因,合并所有差异基因为 NPC 靶点。最后,将白屈菜相关靶点与 NPC 相关靶点通过生信在线工具(<http://bioinformatics.psb.ugent.be/webtools/Venn/>)进行韦恩图映射,获得白屈菜治疗 NPC 作用的交集靶点。

表 1 GEO 数据库中与 NPC 相关的数据组数据集

GSE ID 号	正常/个	肿瘤/个
GSE68799	4	42
GSE118719	4	7
GSE134884	3	3

1.3 白屈菜治疗 NPC 模块靶点的筛选及其 PPI 网络构建

将映射后获得的白屈菜治疗 NPC 作用的交集靶点,在 STRING 数据库中获得靶点-靶点功能相关蛋白间的网络相互作用关系,选择的最小相互作用得分>0.700,得到靶点 PPI 网络图及其 tsv 数据。运用 Cytoscape 3.7.1 中 network analyzer,分析网络中自由度中位数和最大自由度等拓扑参数,选取 degree

前 10 的靶点作为核心靶点。

1.4 靶点的 GO 和 KEGG 通路富集分析

应用 R 语言 V4.1.3 中的“ClusterProfiler”等 R 包,对获得的核心靶点进行 GO 分析、KEGG 通路富集分析及可视化,基因注释信息来自“org.Hs.eg.Db”,富集时的 p-value Cutoff=0.05, q-value-Cutoff=0.05。

1.5 分子对接

通过分子对接可以预测蛋白与小分子的结合能力。白屈菜的结构从 PubChem 数据库(<https://pubchem.ncbi.nlm.nih.gov/>)获取,对应的蛋白结构从 PDB 数据库(<https://www.rcsb.org/>)获得。通过 Chem Bio Office 软件中的 3D Draw 模块将白屈菜活性成分结构进行最小能 MM2 力场优化,通过 Raccoon 软件转化为 PDBQT。通过 Autodock Vina 软件的配套工具 MGLTools 1.5.6 处理蛋白,加氢,Gasteiger 电荷,合并非极性氢等操作,保存 pdbqt 格式,为配体对接做好准备。

1.6 实验验证

1.6.1 细胞株 人 NPC 细胞株 5-8F 购自商城北纳创联生物科技有限公司,由本实验室传代培养。

1.6.2 药物与试剂 对照品血根碱(货号:B21412-20 mg,质量分数 $\geq 98\%$)、白屈菜红碱(货号:B20052-20 mg,质量分数 $\geq 98\%$)均购自上海源叶生物科技有限公司;5-氟尿嘧啶(大连美仑生物技术有限公司,货号:51-21-8);RPMI 1640 培养基(美国 HyClone 公司,货号:PM150110);胎牛血清(美国 Gibco 公司,货号:04-001-1A);噻唑蓝(货号:M8180)、marker(货号:PR1910-100T)均购自北京索莱宝科技有限公司;Annexin V-FITC/PI 荧光双染细胞凋亡检测试剂盒(武汉伊莱瑞特生物科技股份有限公司,货号:VBD53M1ZL3);BCA 蛋白定量试剂盒(杭州联科生物科技股份有限公司,货号:70-PQ0012);脱脂奶粉[生工生物工程(上海)股份有限公司,货号:A600669-0250];顺铂(美国 Sigma 公司,批号:MKCM2435);蛋白激酶 B (protein kinase B,AKT)(货号:60203-2-Ig)、磷脂酰肌醇三激酶 (phosphatidylinositol 3-Kinase, PI3K)(货号:00070453)、GAPDH(货号:00113797)、 β -actin(货号:10024215)购自美国 Proteintech 公司;ERK1/2(美国 Cell Signaling Technology 公司,货号:4695S);PCNA(北京博奥森生物技术有限公司,批号:AH08154079);Goat anti-Mouse 二抗(货号:926-68070)、Goat anti-Rabbit 二抗(货号:926-32211)均购自美国 Licor 公司。

1.6.3 主要仪器 倒置显微镜(日本 Olympus 公司,

型号:CKX31);CO₂培养箱(上海赛默飞世尔公司,型号:HERAcell150i);微孔板分光光度计(美国 Biotek 公司,型号:800TS);双荧光细胞分析仪(美国 Nexcelom 公司,型号:Cellometer K2);高速冷冻离心机(美国 Beckman Coulter 公司,型号:Microfuge 20R);多功能荧光成像仪(美国 Licor 公司,型号:Odyssey CLX);蓝箭快转仪(广州道一科学技术有限公司,型号:FTB95);电泳仪(北京君意东方电泳设备有限公司,型号:JY600HE)。

1.6.4 MTT 法检测细胞增殖能力 采用 MTT 实验法检测白屈菜主要活性成分中具有明显抗肿瘤作用的血根碱、白屈菜红碱对 NPC 细胞增殖的影响。取对数生长周期的 5-8F 细胞,用胰酶消化后收集细胞(5×10^3 个/孔)接种于 96 孔培养板中,于细胞培养箱中培养 7 h。待细胞贴壁后,吸弃原培养液,分别加入不同的含药培养液培养处理 24 h 和 48 h 后,吸弃上清液,每孔加入 100 μ L MTT 工作液,37 $^{\circ}$ C 避光培养 4 h,再次弃上清液,加入 100 μ L DMSO,避光摇晃 10 min 后,用酶标仪检测 490 nm 波长处 OD 值,计算细胞相对增殖率。细胞相对增殖率=(实验组 OD 值-空白组 OD 值)/(对照组 OD 值-空白组 OD 值) $\times 100\%$ 。

1.6.5 Annexin-V FITC/PI 双荧光染色法检测细胞凋亡 5-8F 细胞经胰酶消化后,将细胞平铺于 6 cm 培养皿,待细胞贴壁后,加入相应的药物,待药物干预细胞 24 h 后,用不含 EDTA 的胰蛋白酶将细胞消化后收集细胞悬液,离心后保留细胞沉淀,然后用 100 μ L 1 \times Blinding buffer 重悬,加入 5 μ L FITC 和 5 μ L PI 染液,室温下避光孵育 15 min 后终止染色,采用双荧光细胞分析仪检测细胞凋亡率。

1.6.6 Western blot 法检测相关蛋白表达水平 采用 Western blot 实验检测白屈菜主要活性成分中具有明显抗肿瘤作用的血根碱、白屈菜红碱对 NPC 细胞的影响。设置血根碱 5 μ mol \cdot L⁻¹组、白屈菜红碱 5 μ mol \cdot L⁻¹组、溶剂对照组以及阳性对照组(顺铂 4 μ g \cdot mL⁻¹组),处理 24 h 后,在冰上使用 PBS 清洗细胞,再向培养皿中加入 RIPA 裂解液,用细胞刮收集细胞碎片,置于离心管内。4 $^{\circ}$ C 裂解 30 min 后,将离心管置于提前预冷的离心机中按 12 000 r/min 离心 10 min,收集上清液。按照 BCA 蛋白浓度测定试剂盒说明书操作,测定蛋白浓度。按 60 μ g 上样量配制样品并变性。于 SDS-PAGE 凝胶电泳按 40 V,分离后 6 h,采用半干转膜仪转膜 20 min。用 5% 的脱脂牛奶封闭

1 h,加入一抗 XIAP(1:1 000)、PCNA(1:1 000)、ERK1/2(1:1 000)和 AKT(1:1 000)孵育过夜,第 2 天洗膜后,避光孵育荧光二抗(1:10 000)2 h,洗膜,最后在 Odyssey 多功能荧光成像仪成像,Image studio 软件框选条带信号值。

1.7 统计学分析

采用 SPSS 26.0 统计软件处理,计量资料实验数据服从正态分布,数据以“ $\bar{x} \pm s$ ”表示。单因素设计和多组间计量资料比较采用单因素方差分析,多重比较则采用 LSD 法, $P < 0.05$ 认为差异有统计学意义。结果分析图由 GraphPad Prism 8.0 软件制作完成。

2 结果

2.1 白屈菜活性成分和作用靶点筛选

如图 1 所示,根据限制条件对 TCMSp、BATMAN-TCM 数据库中白屈菜活性成分进行检索,去掉重复成分后共得到 37 个生物活性成分,通过 SwissTargetPrediction 等数据库检索药物靶点,去除重复项后经 UniProt 数据库矫正得到 1 419 个白屈菜靶点。

2.2 白屈菜治疗 NPC 作用靶点筛选及其 PPI 网络

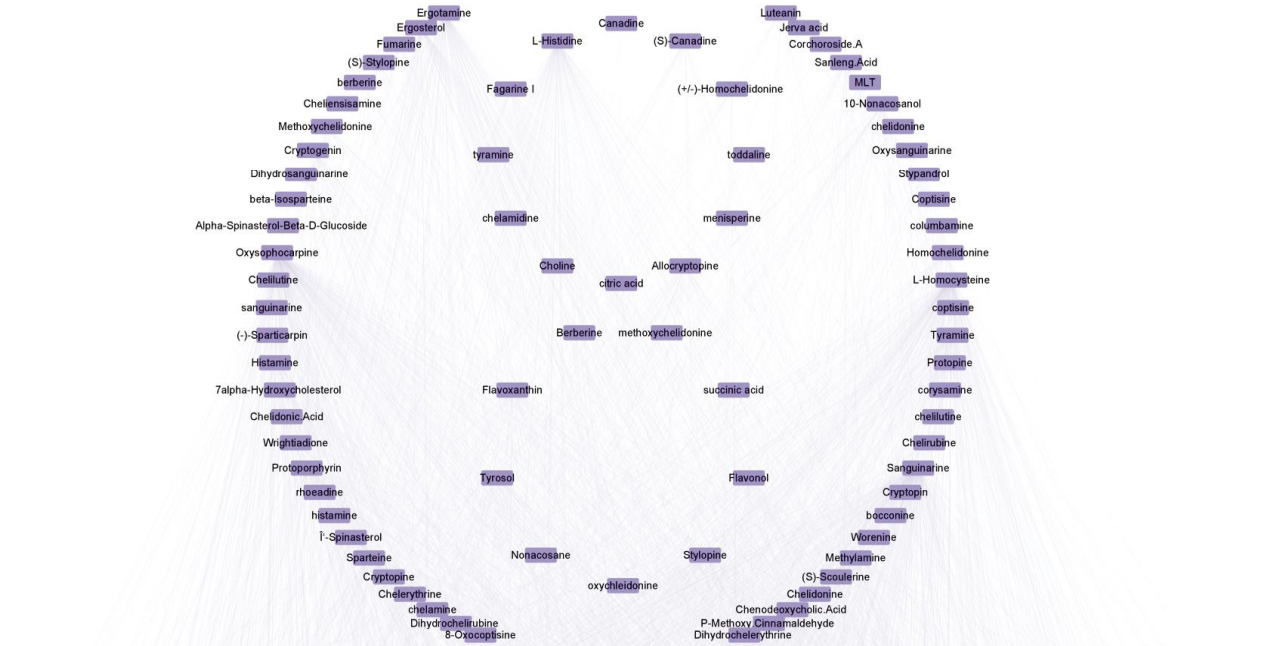
检索 GEO 数据库,共收集到 7 852 个 NPC 疾病基因,通过生信在线工具获得白屈菜与 NPC 的交集靶点共 327 个,详见图 2。同时,应用 STRING 数据库收集 327 个靶点功能相关的 PPI 数据,构建白屈菜治疗 NPC 靶点及其功能相关 PPI 网络。详见图 3。

2.3 PPI 网络拓扑参数分析及核心靶点筛选

将映射得到的交集蛋白导入 Cytoscape 3.7.1,计算白屈菜抗 NPC 靶点及功能相关 PPI 网络的拓扑参数,可得靶点自由度的中位数为 5.662,最大自由度为 48,前 10 个核心靶点分别为:EGFR、TP53、VEGFA、TNF、FN1、MMP9、JUN、FGF2、LYN、F2。核心靶点对应的活性成分如图 4 所示,主要活性成分包括:血根碱、白屈菜红碱、鹅去氧胆碱和氧化槐果碱等。

2.4 核心靶点的 GO 分析和 KEGG 通路富集分析

通过 R 语言相关的包对核心靶点进行 GO 富集分析。其中,生物过程(biological processes, BP)主要涉及创伤治愈、神经发生调控和神经系统发育调控。细胞组分(cellular component, CC)主要涉及囊泡腔、膜筏、膜微区和含胶原的细胞外基质。分子功能(molecular function, MF)主要涉及泛素蛋白连接酶结合、硫化物结合、整合素结合、肝素结合和糖胺聚糖结合。详见图 5。KEGG 信号通路主要富集到 MAPK 信号通路、PI3K/AKT 信号通路。详见图 6。



HUP65 DRD1 PPR2R1A KIT SORBS3 BMP5 NARS FAN52 GABRA3PDGFR1 SIX1 SERPINA3CHRM2 MTRN1ADNAJ3 DDC LEP ATP13A2 SOX9 RARFGE2CHRM5 GRM7 CDK15 HTR30 COX1 ALDH2A NAE1 NGFR GAPDH TPM1 F5 CDK5R1HIST1H1GQTRAP MGR4 ITGAV GLYT1L1
 CAP2B PTGDR2 BCL2 TNK2PPARGC11BHS1 KGN2 QG1 GORASP2AMP2 TRX5 MCM3 SQN4CACNATA KIF14 CEP44 SMOX BIGD1 HTR2A SAMO5LABG11 IL13 GABRG PPP2CABLES1 SRR POLB KRT133MARCD CD300A DCXR CKB NDUFS2AMCA1 STP1 PDE4D ADAP1
 PPH1R18BQLAP DQOUK SHBG UBE2B TRH KRT9 BARD1 ADA SULT1E1 E1E3F CHAT MYL4 AMB5XRC06P4EST55 VM9 F13A1 CPNE1 BMP6 HDACS2CYP27B2CYSLTR2 HIBCH ABAT MAOB HBB HSP90ABEHRNA9 DQJ3 P9P5C KYNU CACNA11PK3CA AVPR2 TBK1 AQP1
 RAB38 ITG52 GATA3 SARS2 AREG ADAM11DABCC8 HMG2A OXER1 CABP8 EPDR ZNF292SNK2A1PDE1CCACNA1CACSS1SERPINE2CXOZC ERP44 HSPA2 RPSA CRT2 CTSL EIF2AK1 GALK1 SLC25A2 CD34 ACSL1 SDHA HTR1A AVPR1B LCM22 FXN EDA TNFAIP3 LYN ACRY1
 NFKB1 SLC7A1 SLC7A8 HIBADH NUDT1ACNA1DABCC8 HMG2A OXER1 CABP8 EPDR ZNF292SNK2A1PDE1CCACNA1CACSS1SERPINE2CXOZC ERP44 HSPA2 RPSA CRT2 CTSL EIF2AK1 GALK1 SLC25A2 CD34 ACSL1 SDHA HTR1A AVPR1B LCM22 FXN EDA TNFAIP3 LYN ACRY1
 GSTA4 TQPI TALD01 TACT1 SRI SLC6A8 PAICS PROS1 GG11 ITG5B ADH1A IQG2 CYP19A1 CPB2 GRIN2B PDE6C SLC17A7SHRHP GSTP1MTHFD1L MGS9 DRD4 SLC36A1 CDG42 GABBR1PDZRN4 LYZ FADS1 GRP5 THRAPP3CHRNA4 GSTM3 ABCG9 RXFP4TXNDG12KDM68 BAG5
 FDP5 GADL1ADRA1DCYR1B1 PLD1 PDGCD2 VTN CHRNA6 TET1 CYP2R1 GUC2 CACNA1QOTCH1 OTIC CHRN9UG13A1 HGFAC FABP3 MTHFD1 FH ACSL4 DARS DGKI KDR PAK8 PROZ TGF3 SHH CBR1 SLC25A10 AKT1 PDE11A CTR9 ST13 DARS2 CACNB2ZYP11A1
 RARG MAPK1 SMO ABCG2 DICER1 BMP4 GRIN2DPDGFRAATP1A1 SCN3B LINC7 PDE3B DKK3 TREM1 SLC6A5 CNR2 IPOT ATP5A1 SNW1 GPX7 GLO1 NQO2 XRCO4 VDR FARS2 SLC7A7 MOC52 F7 CSAD SLC7A3PPP2CB CDH3 POLA2 PPP3R1SLC22A5 PCK56 GPX6
 RTN2 ZEB2 KRT10 DMW0 BQHE PTGFR NR1H2 ADRA2BPTGER4SULT2BACNA1KCNB1 NPHS1 SCN11A BIRC5 IGFBP5 CPT1A HMTT PPP6R2PLA2G1NOS1AP ZP3 PDE4C S100G HRC PDXK AMHR2 ESD WLS NTS6 MGST3 PHLFP1 C6 PANX1 HSPA8 CTR AFM
 HPGD5 SH3BP5SULCLG2 KCN2D SREBF2CYP24A RNASE1 PINK1 MST1R CHRNA3 ABCA1 JUP KCM2K ABCG1KIAA2032CLCA2 TH GAMT CY5B SCN2B SSU72 KLF4 FOSL3 JARID2 DRY30 8-MW S100A13 NNMT ACHE H1D BDKR62 NAV2 PDE9A TOX3 HMGCRKMT1B GRIA2
 SRD5A2SERPINC1GFBP3 CXMT2 USP4A APOH FGFRI1 AHSO CHRNE AKR1B1 TH1 P10XK PTGER3ONMT3A BMP2 PRMT1 GRIN2A SLC6A5 KDNK4 LRPI GSR SLC25A6 MEDI TAAR1 FOXP3KORC1L2NM13B GATM F12 SRAO3 PROCR CHRNA7 KCM4 P853 RUMBL2 GRLH ITGA2B
 RGS2 CHRN2 CAT HTR1B ACE OPRD1 SLC6R 2Mw SLC18A2FVB1B ALA52 SLA2 OSTO2 GAS6 TASH1R3 GRB2 COP92 ASPH CCL3 SF3B3 IMPA1 CYP27A1 LTC4S L3 YWHAH GSTA1 SLC19A3ATP8V1AKCN3 MAPK14 GSTR1 HDAC2 USP46 RYR2 FECH HMT1
 COX5A ITGA2 HSPB1 ATCAY1 GDC0C4 TASH1R1 ORB2CHDRS3 DRIN3B AKR1C3 APLN TUBA1A NR4A3 TA2A ABL1 PCDH1HSD11B1 CKM C3 GOT1L1 FLNA C1QTNF3KNA23PDE88 PPP2CB KCM5CHRNA104DCY3 HAL FAH CTA6E5 PPK63CYSLTR1SQN2A ADYR1 SDB FTCD
 ADSS CHRNA3 PDE2A NDUFC2CAP2A1 PIK3CG NDUFA5 NEFH ABCB4 HSP4 CETN1CBFA2T3 HAGH SGOL2 POLA1 CS13 GPX8 CETN3 ZNF232 NQO1 C1QTNF3KPK36 NARS2 PTGK2 CHRNA2ATP254 PTPG51 PRKCD PPP6R1 IRE2B WNT10BADSLL1ACVBR1B SNA2 MTAP SLC32A1 EGFR
 SLC18A1 SDSL GPHN SQNSA ACSL3 GLRA1HSP90AACN3B TTH1 NEDD4 ARRB2 PRDX4 GGT6 ABCG1 CHRNA2 IL1B HGD GPRC5A ANXA1 GABRG3 ARRB1 ANK3 PALM SERPINE1 CTH HTR6 GRIN1SERPINB6 GJA1 GSK3A GCMT PTFN2 GABR2 RCHY1 FKBP1A HCK RYR1
 GRIK2 FGF18 CALB1 APOC1 CBSL AIF1 C2orf83 SCN9A GNAS CDH8 BCAT2 AMDHD1 SORT1 HARSHOSPHOGNAT3 NRPB ESRRA PAHA1 FNT RAB8B P3H5 AKR1D1SLC38A7 CABP1ALOX5AP SMS BHMT ADORA2A RORA TSNAX PDCD1 COX2 DDR1 SCN1B GLUD1 GOLT2
 AFG3L2 LDB1 SLC19A3 CAV2 MGS11 STK17B CRAT FGF1 SULF2 DGKG GPX3 CACNA1FADRBK2COL4A4 U2SR2 ME2 CACNA1F6ABRA5 IRKKG SEC14L4SHMT2 SLC44A4CRH1R1 SLC1A5 WNT5A SLC6A4 HCAR3HOMER1 IL10 SERPINB3SCRIB CRZY CE8P6 KLK3 ARG2 LRRC6A F2RL1
 NRD1 ZNF936 EPHX2 MOC53 ETHE1 CP NR1H3 SQRLD SOCS1 ABCG2 CAR52 ADRA2C KARS ADRA1A CHRNA4 CASP3 PRKCG DTNBP1 PARK2 F2R ABHD5 1-MW AVPR1A ALAD LDLR SRC STAR ANG PGR PARO1 SH1 PIM1 GABRG1 CBS REC4 PGRMC1 NEFL
 TTRAL CE2N2 AARS PAH FAM175A PKR1 NR1H3 MTRF1 CSE1 PDE4A HTR3B GSTA3 F2 DUSP6 ATM BHMT2 APOC3 RLF ADORA2BHADHA PRIF CACNA1S AP1P CSE1R RPN1 HTR5A FGE23 HTR1E F9 AP1M1 AMPD3 ALOX5 G5TM1 ESR1 PPP3R2 GCLC
 PEO3 PRS12 SIRT2 CASP1 SPP1 NQOR2 CASK ATF4 PNMT COX7A1 NFE51 PTK2 WNT4 CARS SPAST NTCO1A GAD1 LEF1 RELB NMUR2SLC23A1 ASH1A1 ADH5 E1O SIRT4 SRM ATP1A3 UBA3 AHGY1 NTRK2 MOC53 MMP28 TTR MTRR HXK FTSJ1 ATP1C
 P2RY1 CALM2 SELF APLP1 DNM3 LIPIA AGT SACS RNF41 LDB3 CDK1CHRAM7BNAJ1 PSAT1 FARS8 PPARA GAD1 RSPD1 QLR2A SHCBP1PCY17B UROS P2RX7 GGT5 APAF1 NPEPPSP3C4ERUDADRA2A NCOA2 SLC6A2 PPR6R3 F8 ALK ALC1A1 ORP1M
 P2RX2 ARPN APOC2 PTPN14 PRKDC HTR2B CAMK2C TREV3 BABAM1 CES2 GRIN2C TTPA CRH GABRP HDB PRKCA MS4A2 CHKB FCER2G UBA1 A5T1 GRAP2 CDK6 CAMLG CAMTA12NF219 TYR PPARG DOST2 S10A02 GMS7 FARSA HTR3C HTR7 HSD17BENOPH1SORCS3
 ME3 DRD5 SCN3A KPN2H MOC51 PIKRS1 HOKA10 POR IARS COLQ ADCY5 GPR16 NR3C2 DMPK PDE8A OAZ1 PLA2G4F DRD2 YARS GSTB1 HPK1 ARD1AMARXBP3 SYT2 COX41TRMT1VDW77 DMD DGT01 PLAU COMT G95 GABRE ARBDC3 C5 VTI1A GRI3
 FGA F11 CTSB KRR1 KIF1G CAMK2D COFA CFH ASRGL1 NTS62 PLD2 F2RL2 M3AR NUDT9 PRKAB1 G0T1 STOX1 ADCY1 ERM2A CASP8 SOAT1 FGF2 PDE7A ASH5 OTTRD1 AARS2 SETX SLC39A7 REN YARS2 SOAT2 ATP2A1SECH4L2 TRAF2 HNR2B MCR4
 GPK2 CTSB GABRA1 SLC6A1 L4 HROB1 PML RARRES HUIE1 COX6C HCN4 TMM1 TASH1R2L1CB3 FEZF2 CALCA PQL5 THN5L1 REST ADH1B ADRE2 PAH2 GURS PLAG1 RYR3 NR1H4 OGDH GFAPPARGC1A DDO GSTM4 MTRN1B ARGE ALDH1A1 G0T7 FABP5 GBS
 PIK3R3 DERL1 TOP2A ODC1 GRIN3A VCAM1 DHDH F2RL3 ACO1 MGS12 P2RX3 RARB LANCL2 PDE8A DPPA3 CX3CR1 CALM3 PPM1G NQ52 COL1A1 CCL5 AKR1C2GABRR1 NR1H2 ESR2 COX7B MTR SCN1A DRD3 PDE7B KRT6A RXRA AOC3 ADRB1 ANMT GABRG2 NCBP2
 METAP2 ZFPM1 PNPLA2 PNPO KCM18 GLYATL2AGX72 SECL4L3MTHF5 MAD2L2 HSPA4 SHMT1 GPT FAM175BKNK31 PDE5A RANBP2 GP1BA ADAP2 HIFA UROCI1 PUG ADH1C ITPR2 OXTR SLC6A3R1TARS SERPINB3CALM1 SIX4 HRH4 CDK5R2 KONA1 F3 CSF2 LTA ADNP
 RIK1 PIK3CD ACVR1L HNF1B GGCX PCDY1BCARTPT PEKP SHANK1ZRNAN3 GC NR1P CXCL13 CHGA BCL11B PHB COX7B2 VARS NOTCH2 LILRB1 CPB1 TAL1 TNCC1 IGH15 PRKCB CHRNA5 IDNK NR1P2 HTR6 HTR2B HTR1E HTR2A HTR2B HTR2C HTR2D HTR2E HTR2F HTR2G HTR2H HTR2I HTR2J HTR2K HTR2L HTR2M HTR2N HTR2O HTR2P HTR2Q HTR2R HTR2S HTR2T HTR2U HTR2V HTR2W HTR2X HTR2Y HTR2Z HTR2AA HTR2AB HTR2AC HTR2AD HTR2AE HTR2AF HTR2AG HTR2AH HTR2AI HTR2AJ HTR2AK HTR2AL HTR2AM HTR2AN HTR2AO HTR2AP HTR2AQ HTR2AR HTR2AS HTR2AT HTR2AU HTR2AV HTR2AW HTR2AX HTR2AY HTR2AZ HTR2BA HTR2BB HTR2BC HTR2BD HTR2BE HTR2BF HTR2BG HTR2BH HTR2BI HTR2BJ HTR2BK HTR2BL HTR2BM HTR2BN HTR2BO HTR2BP HTR2BQ HTR2BR HTR2BS HTR2BT HTR2BU HTR2BV HTR2BW HTR2BX HTR2BY HTR2BZ HTR2CA HTR2CB HTR2CC HTR2CD HTR2CE HTR2CF HTR2CG HTR2CH HTR2CI HTR2CJ HTR2CK HTR2CL HTR2CM HTR2CN HTR2CO HTR2CP HTR2CQ HTR2CR HTR2CS HTR2CT HTR2CU HTR2CV HTR2CW HTR2CX HTR2CY HTR2CZ HTR2DA HTR2DB HTR2DC HTR2DD HTR2DE HTR2DF HTR2DG HTR2DH HTR2DI HTR2DJ HTR2DK HTR2DL HTR2DM HTR2DN HTR2DO HTR2DP HTR2DQ HTR2DR HTR2DS HTR2DT HTR2DU HTR2DV HTR2DW HTR2DX HTR2DY HTR2DZ HTR2EA HTR2EB HTR2EC HTR2ED HTR2EE HTR2EF HTR2EG HTR2EH HTR2EI HTR2EJ HTR2EK HTR2EL HTR2EM HTR2EN HTR2EO HTR2EP HTR2EQ HTR2ER HTR2ES HTR2ET HTR2EU HTR2EV HTR2EW HTR2EX HTR2EY HTR2EZ HTR2FA HTR2FB HTR2FC HTR2FD HTR2FE HTR2FF HTR2FG HTR2FH HTR2FI HTR2FJ HTR2FK HTR2FL HTR2FM HTR2FN HTR2FO HTR2FP HTR2FQ HTR2FR HTR2FS HTR2FT HTR2FU HTR2FV HTR2FW HTR2FX HTR2FY HTR2FZ HTR2GA HTR2GB HTR2GC HTR2GD HTR2GE HTR2GF HTR2GG HTR2GH HTR2GI HTR2GJ HTR2GK HTR2GL HTR2GM HTR2GN HTR2GO HTR2GP HTR2GQ HTR2GR HTR2GS HTR2GT HTR2GU HTR2GV HTR2GW HTR2GX HTR2GY HTR2GZ HTR2HA HTR2HB HTR2HC HTR2HD HTR2HE HTR2HF HTR2HG HTR2HH HTR2HI HTR2HJ HTR2HK HTR2HL HTR2HM HTR2HN HTR2HO HTR2HP HTR2HQ HTR2HR HTR2HS HTR2HT HTR2HU HTR2HV HTR2HW HTR2HX HTR2HY HTR2HZ HTR2IA HTR2IB HTR2IC HTR2ID HTR2IE HTR2IF HTR2IG HTR2IH HTR2II HTR2IJ HTR2IK HTR2IL HTR2IM HTR2IN HTR2IO HTR2IP HTR2IQ HTR2IR HTR2IS HTR2IT HTR2IU HTR2IV HTR2IW HTR2IX HTR2IY HTR2IZ HTR2JA HTR2JB HTR2JC HTR2JD HTR2JE HTR2JF HTR2JG HTR2JH HTR2JI HTR2JJ HTR2JK HTR2JL HTR2JM HTR2JN HTR2JO HTR2JP HTR2JQ HTR2JR HTR2JS HTR2JT HTR2JU HTR2JV HTR2JW HTR2JX HTR2JY HTR2JZ HTR2KA HTR2KB HTR2KC HTR2KD HTR2KE HTR2KF HTR2KG HTR2KH HTR2KI HTR2KJ HTR2KK HTR2KL HTR2KM HTR2KN HTR2KO HTR2KP HTR2KQ HTR2KR HTR2KS HTR2KT HTR2KU HTR2KV HTR2KW HTR2KX HTR2KY HTR2KZ HTR2LA HTR2LB HTR2LC HTR2LD HTR2LE HTR2LF HTR2LG HTR2LH HTR2LI HTR2LJ HTR2LK HTR2LM HTR2LN HTR2LO HTR2LP HTR2LQ HTR2LR HTR2LS HTR2LT HTR2LU HTR2LV HTR2LW HTR2LX HTR2LY HTR2LZ HTR2MA HTR2MB HTR2MC HTR2MD HTR2ME HTR2MF HTR2MG HTR2MH HTR2MI HTR2MJ HTR2MK HTR2ML HTR2MN HTR2MO HTR2MP HTR2MQ HTR2MR HTR2MS HTR2MT HTR2MU HTR2MV HTR2MW HTR2MX HTR2MY HTR2MZ HTR2NA HTR2NB HTR2NC HTR2ND HTR2NE HTR2NF HTR2NG HTR2NH HTR2NI HTR2NJ HTR2NK HTR2NL HTR2NM HTR2NO HTR2NP HTR2NQ HTR2NR HTR2NS HTR2NT HTR2NU HTR2NV HTR2NW HTR2NX HTR2NY HTR2NZ HTR2OA HTR2OB HTR2OC HTR2OD HTR2OE HTR2OF HTR2OG HTR2OH HTR2OI HTR2OJ HTR2OK HTR2OL HTR2OM HTR2ON HTR2OO HTR2OP HTR2OQ HTR2OR HTR2OS HTR2OT HTR2OU HTR2OV HTR2OW HTR2OX HTR2OY HTR2OZ HTR2PA HTR2PB HTR2PC HTR2PD HTR2PE HTR2PF HTR2PG HTR2PH HTR2PI HTR2PJ HTR2PK HTR2PL HTR2PM HTR2PN HTR2PO HTR2PP HTR2PQ HTR2PR HTR2PS HTR2PT HTR2PU HTR2PV HTR2PW HTR2PX HTR2PY HTR2PZ HTR2QA HTR2QB HTR2QC HTR2QD HTR2QE HTR2QF HTR2QG HTR2QH HTR2QI HTR2QJ HTR2QK HTR2QL HTR2QM HTR2QN HTR2QO HTR2QP HTR2QQ HTR2QR HTR2QS HTR2QT HTR2QU HTR2QV HTR2QW HTR2QX HTR2QY HTR2QZ HTR2RA HTR2RB HTR2RC HTR2RD HTR2RE HTR2RF HTR2RG HTR2RH HTR2RI HTR2RJ HTR2RK HTR2RL HTR2RM HTR2RN HTR2RO HTR2RP HTR2RQ HTR2RR HTR2RS HTR2RT HTR2RU HTR2RV HTR2RW HTR2RX HTR2RY HTR2RZ HTR2SA HTR2SB HTR2SC HTR2SD HTR2SE HTR2SF HTR2SG HTR2SH HTR2SI HTR2SJ HTR2SK HTR2SL HTR2SM HTR2SN HTR2SO HTR2SP HTR2SQ HTR2SR HTR2SS HTR2ST HTR2SU HTR2SV HTR2SW HTR2SX HTR2SY HTR2SZ HTR2TA HTR2TB HTR2TC HTR2TD HTR2TE HTR2TF HTR2TG HTR2TH HTR2TI HTR2TJ HTR2TK HTR2TL HTR2TM HTR2TN HTR2TO HTR2TP HTR2TQ HTR2TR HTR2TS HTR2TT HTR2TU HTR2TV HTR2TW HTR2TX HTR2TY HTR2TZ HTR2UA HTR2UB HTR2UC HTR2UD HTR2UE HTR2UF HTR2UG HTR2UH HTR2UI HTR2UJ HTR2UK HTR2UL HTR2UM HTR2UN HTR2UO HTR2UP HTR2UQ HTR2UR HTR2US HTR2UT HTR2UU HTR2UV HTR2UW HTR2UX HTR2UY HTR2UZ HTR2VA HTR2VB HTR2VC HTR2VD HTR2VE HTR2VF HTR2VG HTR2VH HTR2VI HTR2VJ HTR2VK HTR2VL HTR2VM HTR2VN HTR2VO HTR2VP HTR2VQ HTR2VR HTR2VS HTR2VT HTR2VU HTR2VV HTR2VW HTR2VX HTR2VY HTR2VZ HTR2WA HTR2WB HTR2WC HTR2WD HTR2WE HTR2WF HTR2WG HTR2WH HTR2WI HTR2WJ HTR2WK HTR2WL HTR2WM HTR2WN HTR2WO HTR2WP HTR2WQ HTR2WR HTR2WS HTR2WT HTR2WU HTR2WV HTR2WW HTR2WX HTR2WY HTR2WZ HTR2XA HTR2XB HTR2XC HTR2XD HTR2XE HTR2XF HTR2XG HTR2XH HTR2XI HTR2XJ HTR2XK HTR2XL HTR2XM HTR2XN HTR2XO HTR2XP HTR2XQ HTR2XR HTR2XS HTR2XT HTR2XU HTR2XV HTR2XW HTR2XX HTR2XY HTR2XZ HTR2YA HTR2YB HTR2YC HTR2YD HTR2YE HTR2YF HTR2YG HTR2YH HTR2YI HTR2YJ HTR2YK HTR2YL HTR2YM HTR2YN HTR2YO HTR2YP HTR2YQ HTR2YR HTR2YS HTR2YT HTR2YU HTR2YV HTR2YW HTR2YX HTR2YY HTR2YZ HTR2ZA HTR2ZB HTR2ZC HTR2ZD HTR2ZE HTR2ZF HTR2ZG HTR2ZH HTR2ZI HTR2ZJ HTR2ZK HTR2ZL HTR2ZM HTR2ZN HTR2ZO HTR2ZP HTR2ZQ HTR2ZR HTR2ZS HTR2ZT HTR2ZU HTR2ZV HTR2ZW HTR2ZX HTR2ZY HTR2ZZ HTR2AA HTR2AB HTR2AC HTR2AD HTR2AE HTR2AF HTR2AG HTR2AH HTR2AI HTR2AJ HTR2AK HTR2AL HTR2AM HTR2AN HTR2AO HTR2AP HTR2AQ HTR2AR HTR2AS HTR2AT HTR2AU HTR2AV HTR2AW HTR2AX HTR2AY HTR2AZ HTR2BA HTR2BB HTR2BC HTR2BD HTR2BE HTR2BF HTR2BG HTR2BH HTR2BI HTR2BJ HTR2BK HTR2BL HTR2BM HTR2BN HTR2BO HTR2BP HTR2BQ HTR2BR HTR2BS HTR2BT HTR2BU HTR2BV HTR2BW HTR2BX HTR2BY HTR2BZ HTR2CA HTR2CB HTR2CC HTR2CD HTR2CE HTR2CF HTR2CG HTR2CH HTR2CI HTR2CJ HTR2CK HTR2CL HTR2CM HTR2CN HTR2CO HTR2CP HTR2CQ HTR2CR HTR2CS HTR2CT HTR2CU HTR2CV HTR2CW HTR2CX HTR2CY HTR2CZ HTR2DA HTR2DB HTR2DC HTR2DD HTR2DE HTR2DF HTR2DG HTR2DH HTR2DI HTR2DJ HTR2DK HTR2DL HTR2DM HTR2DN HTR2DO HTR2DP HTR2DQ HTR2DR HTR2DS HTR2DT HTR2DU HTR2DV HTR2DW HTR2DX HTR2DY HTR2DZ HTR2EA HTR2EB HTR2EC HTR2ED HTR2EE HTR2EF HTR2EG HTR2EH HTR2EI HTR2EJ HTR2EK HTR2EL HTR2EM HTR2EN HTR2EO HTR2EP HTR2EQ HTR2ER HTR2ES HTR2ET HTR2EU HTR2EV HTR2EW HTR2EX HTR2EY HTR2EZ HTR2FA HTR2FB HTR2FC HTR2FD HTR2FE HTR2FF HTR2FG HTR2FH HTR2FI HTR2FJ HTR2FK HTR2FL HTR2FM HTR2FN HTR2FO HTR2FP HTR2FQ HTR2FR HTR2FS HTR2FT HTR2FU HTR2FV HTR2FW HTR2FX HTR2FY HTR2FZ HTR2GA HTR2GB HTR2GC HTR2GD HTR2GE HTR2GF HTR2GG HTR2GH HTR2GI HTR2GJ HTR2GK HTR2GL HTR2GM HTR2GN HTR2GO HTR2GP HTR2GQ HTR2GR HTR2GS HTR2GT HTR2GU HTR2GV HTR2GW HTR2GX HTR2GY HTR2GZ HTR2HA HTR2HB HTR2HC HTR2HD HTR2HE HTR2HF HTR2HG HTR2HH HTR2HI HTR2HJ HTR2HK HTR2HL HTR2HM HTR2HN HTR2HO HTR2HP HTR2HQ HTR2HR HTR2HS HTR2HT HTR2HU HTR2HV HTR2HW HTR2HX HTR2HY HTR2HZ HTR2IA HTR2IB HTR2IC HTR2ID HTR2IE HTR2IF HTR2IG HTR2IH HTR2II HTR2IJ HTR2IK HTR2IL HTR2IM HTR2IN HTR2IO HTR2IP HTR2IQ HTR2IR HTR2IS HTR2IT HTR2IU HTR2IV HTR2IW HTR2IX HTR2IY HTR2IZ HTR2JA HTR2JB HTR2JC HTR2JD HTR2JE HTR2JF HTR2JG HTR2JH HTR2JI HTR2JJ HTR2JK HTR2JL HTR2JM HTR2JN HTR2JO HTR2JP HTR2JQ HTR2JR HTR2JS HTR2JT HTR2JU HTR2JV HTR2JW HTR2JX HTR2JY HTR2JZ HTR2KA HTR2KB HTR2KC HTR2KD HTR2KE HTR2KF HTR2KG HTR2KH HTR2KI HTR2KJ HTR2KK HTR2KL HTR2KM HTR2KN HTR2KO HTR2KP HTR2KQ HTR2KR HTR2KS HTR2KT HTR2KU HTR2KV HTR2KW HTR2KX HTR2KY HTR2KZ HTR2LA HTR2LB HTR2LC HTR2LD HTR2LE HTR2LF HTR2LG HTR2LH HTR2LI HTR2LJ HTR2LK HTR2LM HTR2LN HTR2LO HTR2LP HTR2LQ HTR2LR HTR2LS HTR2LT HTR2LU HTR2LV HTR2LW HTR2LX HTR2LY HTR2LZ HTR2MA HTR2MB HTR2MC HTR2MD HTR2ME HTR2MF HTR2MG HTR2MH HTR2MI HTR2MJ HTR2MK HTR2ML HTR2MN HTR2MO HTR2MP HTR2MQ HTR2MR HTR2MS HTR2MT HTR2MU HTR2MV HTR2MW HTR2MX HTR2MY HTR2MZ HTR2NA HTR2NB HTR2NC HTR2ND HTR2NE HTR2NF HTR2NG HTR2NH HTR2NI HTR2NJ HTR2NK HTR2NL HTR2NM HTR2NO HTR2NP HTR2NQ HTR2NR HTR2NS HTR2NT HTR2NU HTR2NV HTR2NW HTR2NX HTR2NY HTR2NZ HTR2OA HTR2OB HTR2OC HTR2OD HTR2OE HTR2OF HTR2OG HTR2OH HTR2OI HTR2OJ HTR2OK HTR2OL HTR2OM HTR2ON HTR2OO HTR2OP HTR2OQ HTR2OR HTR2OS HTR2OT HTR2OU HTR2OV HTR2OW HTR2OX HTR2OY HTR2OZ HTR2PA HTR2PB HTR2PC HTR2PD HTR2PE HTR2PF HTR2PG HTR2PH HTR2PI HTR2PJ HTR2PK HTR2PL HTR2PM HTR2PN HTR2PO HTR2PP HTR2PQ HTR2PR HTR2PS HTR2PT HTR2PU HTR2PV HTR2PW HTR2PX HTR2PY HTR2PZ HTR2QA HTR2QB HTR2QC HTR2QD HTR2QE HTR2QF HTR2QG HTR2QH HTR2QI HTR2QJ HTR2QK HTR2QL HTR2QM HTR2QN HTR2QO HTR2QP HTR2QQ HTR2QR HTR2QS HTR2QT HTR2QU HTR2QV HTR2QW HTR2QX HTR2QY HTR2QZ HTR2RA HTR2RB HTR2RC HTR2RD HTR2RE HTR2RF HTR2RG HTR2RH HTR2RI HTR2RJ HTR2RK HTR2RL HTR2RM HTR2RN HTR2RO HTR2RP HTR2RQ HTR2RR HTR2RS HTR2RT HTR2RU HTR2RV HTR2RW HTR2RX HTR2RY HTR2RZ HTR2SA HTR2SB HTR2SC HTR2SD HTR2SE HTR2SF HTR2SG HTR2SH HTR2SI HTR2SJ HTR2SK HTR2SL HTR2SM HTR2SN HTR2SO HTR2SP HTR2SQ HTR2SR HTR2SS HTR2ST HTR2SU HTR2SV HTR2SW HTR2SX HTR2SY HTR2SZ HTR2TA HTR2TB HTR2TC HTR2TD HTR2TE HTR2TF HTR2TG HTR2TH HTR2TI HTR2TJ HTR2TK HTR2TL HTR2TM HTR2TN HTR2TO HTR2TP HTR2TQ HTR2TR HTR2TS HTR2TT HTR2TU HTR2TV HTR2TW HTR2TX HTR2TY HTR2TZ HTR2UA HTR2UB HTR2UC HTR2UD HTR2UE HTR2UF HTR2UG HTR2UH HTR2UI HTR2UJ HTR2UK HTR2UL HTR2UM HTR2UN HTR2UO HTR2UP HTR2UQ HTR2UR HTR2US HTR2UT HTR2UU HTR2UV HTR2UW HTR2UX HTR2UY HTR2UZ HTR2VA HTR2VB HTR2VC HTR2VD HTR2VE HTR2VF HTR2VG HTR2VH HTR2VI HTR2VJ HTR2VK HTR2VL HTR2VM HTR2VN HTR2VO HTR2VP HTR2VQ HTR2VR HTR2VS HTR2VT HTR2VU HTR2VV HTR2VW HTR2VX HTR2VY HTR2VZ HTR2WA HTR2WB HTR2WC HTR2WD HTR2WE HTR2WF HTR2WG HTR2WH HTR2WI HTR2WJ HTR2WK HTR2WL HTR2WM HTR2WN HTR2WO HTR2WP HTR2WQ HTR2WR HTR2WS HTR2WT HTR2WU HTR2WV HTR2WW HTR2WX HTR2WY HTR2WZ HTR2XA HTR2XB HTR2XC HTR2XD HTR2XE HTR2XF HTR2XG HTR2XH HTR2XI HTR2XJ HTR2XK HTR2XL HTR2XM HTR2XN HTR2XO HTR2XP HTR2XQ HTR2XR HTR2XS HTR2XT HTR2XU HTR2XV HTR2XW HTR2XX HTR2XY HTR2XZ HTR2YA HTR2YB HTR2YC HTR2YD HTR2YE HTR2YF HTR2YG HTR2YH HTR2YI HTR2YJ HTR2YK HTR2YL HTR2YM HTR2YN HTR2YO HTR2YP HTR2YQ HTR2YR HTR2YS HTR2YT HTR2YU HTR2YV HTR2YW HTR2YX HTR2YY HTR2YZ HTR2ZA HTR2ZB HTR2ZC HTR2ZD HTR2ZE HTR2ZF HTR2ZG HTR2ZH HTR2ZI HTR2ZJ HTR2ZK HTR2ZL HTR2ZM HTR2ZN HTR2ZO HTR2ZP HTR2ZQ HTR2ZR HTR2ZS HTR2ZT HTR2ZU HTR2ZV HTR2ZW HTR2ZX HTR2ZY HTR2ZZ HTR2AA HTR2AB HTR2AC HTR2AD HTR2AE HTR2AF HTR2AG HTR2AH HTR2AI HTR2AJ HTR2AK HTR2AL HTR2AM HTR2AN HTR2AO HTR2AP HTR2AQ HTR2AR HTR2AS HTR2AT HTR2AU HTR2AV HTR2AW HTR2AX HTR2AY HTR2AZ HTR2BA HTR2BB HTR2BC HTR2BD HTR2BE HTR2BF HTR2BG HTR2BH HTR2BI HTR2BJ HTR2BK HTR2BL HTR2BM HTR2BN HTR2BO HTR2BP HTR2BQ HTR2BR HTR2BS HTR2BT HTR2BU HTR2BV HTR2BW HTR2BX HTR2BY HTR2BZ HTR2CA HTR2CB HTR2CC HTR2CD HTR2CE HTR2CF HTR2CG HTR2CH HTR2CI HTR2CJ HTR2CK HTR2CL HTR2CM HTR2CN HTR2CO HTR2CP HTR2CQ HTR2CR HTR2CS HTR2CT HTR2CU HTR2CV HTR2CW HTR2CX HTR2CY HTR2CZ HTR2DA HTR2DB HTR2DC HTR2DD HTR2DE HTR2DF HTR2DG HTR2DH HTR2DI HTR2DJ HTR2DK HTR2DL HTR2DM HTR2DN HTR2DO HTR2DP HTR2DQ HTR2DR HTR2DS HTR2DT HTR2DU HTR2DV HTR2DW HTR2DX HTR2DY HTR2DZ HTR2EA HTR2EB HTR2EC HTR2ED HTR2EE HTR2EF HTR2EG HTR2EH HTR2EI HTR2EJ HTR2EK HTR2EL HTR2EM HTR2EN HTR2EO HTR2EP HTR2EQ HTR2ER HTR2ES HTR2ET HTR2EU HTR2EV HTR2EW HTR2EX HTR2EY HTR2EZ HTR2FA HTR2FB HTR2FC HTR2FD HTR2FE HTR2FF HTR2FG HTR2FH HTR2FI HTR2FJ HTR2FK HTR2FL HTR2FM HTR2FN HTR2FO HTR2FP HTR2FQ HTR2FR HTR2FS HTR2FT HTR2FU HTR2FV HTR2FW HTR2FX HTR2FY HTR2FZ HTR2GA HTR2GB HTR2GC HTR2GD HTR2GE HTR2GF HTR2GG HTR2GH HTR2GI HTR2GJ HTR2GK HTR2GL HTR2GM HTR2GN HTR2GO HTR2GP HTR2GQ HTR2GR HTR2GS HTR2GT HTR2GU HTR2GV HTR2GW HTR2GX HTR2GY HTR2GZ HTR2HA HTR2HB HTR2HC HTR2HD HTR2HE HTR2HF HTR2HG HTR2HH HTR2HI HTR2HJ HTR2HK HTR2HL HTR2HM HTR2HN HTR2HO HTR2HP HTR2HQ HTR2HR HTR2HS HTR2HT HTR2HU HTR2HV HTR2HW HTR2HX HTR2HY HTR2HZ HTR2IA HTR2IB HTR2IC HTR2ID HTR2IE HTR2IF HTR2IG HTR2IH HTR2II HTR2IJ HTR2IK HTR2IL HTR2IM HTR2IN HTR2IO HTR2IP HTR2IQ HTR2IR HTR2IS HTR2IT HTR2IU HTR2IV HTR2IW HTR2IX HTR2IY HTR2IZ HTR2JA HTR2JB HTR2JC HTR2JD HTR2JE HTR2JF HTR2JG HTR2JH HTR2JI HTR2JJ HTR2JK HTR2JL HTR2JM HTR2JN HTR2JO HTR2JP HTR2JQ HTR2JR HTR2JS HTR2JT HTR2JU HTR2JV HTR2JW HTR2JX HTR2JY HTR2JZ HTR2KA HTR2KB HTR2KC HTR2KD HTR2KE HTR2KF HTR2KG HTR2KH HTR2KI HTR2KJ HTR2KK HTR2KL HTR2KM HTR2KN HTR2KO HTR2KP HTR2KQ HTR2KR HTR2KS HTR2KT HTR2KU HTR2KV HTR2KW HTR2KX HTR2KY HTR2KZ HTR2LA HTR2LB HTR2LC HTR2LD HTR2LE HTR2LF HTR2LG HTR2LH HTR2LI HTR2LJ HTR2LK HTR2LM HTR2LN HTR2LO HTR2LP HTR2LQ HTR2LR HTR2LS HTR2LT HTR2LU HTR2LV HTR2LW HTR2LX HTR2LY HTR2LZ HTR2MA HTR2MB HTR2MC HTR2MD HTR2ME HTR2MF HTR2MG HTR2MH HTR2MI HTR2MJ HTR2MK HTR2ML HTR2MN HTR2MO HTR2MP HTR2MQ HTR2MR HTR2MS HTR2MT HTR2MU HTR2MV HTR2MW HTR2MX HTR2MY HTR2MZ HTR2NA HTR2NB HTR2NC HTR2ND HTR2NE HTR2NF HTR2NG HTR2NH HTR2NI HTR2NJ HTR2NK HTR2NL HTR2NM HTR2NO HTR2NP HTR2NQ HTR2NR HTR2NS HTR2NT HTR2NU HTR2NV HTR2NW HTR2NX HTR2NY HTR2NZ HTR2OA HTR2OB HTR2OC HTR2OD HTR2OE HTR2OF HTR2OG HTR2OH HTR2OI HTR2OJ HTR2OK HTR2OL HTR2OM HTR2ON HTR2OO HTR2OP HTR2OQ HTR2OR HTR2OS HTR2OT HTR2OU HTR2OV HTR2OW HTR2OX HTR2OY HTR2OZ HTR2PA HTR2PB HTR2PC HTR2PD HTR2PE HTR2PF HTR2PG HTR2PH HTR2PI HTR2PJ HTR2PK HTR2PL HTR2PM HTR2PN HTR2PO HTR2PP HTR2PQ HTR2PR HTR2PS HTR2PT HTR2PU HTR2PV HTR2PW HTR2PX HTR2PY HTR2PZ HTR2QA HTR2QB HTR2QC HTR2QD HTR2QE HTR2QF HTR2QG HTR2QH HTR2QI HTR2QJ HTR2QK HTR2QL HTR2QM HTR2QN HTR2QO HTR2QP HTR2QQ HTR2QR HTR2QS HTR2QT HTR2QU HTR2QV HTR2QW HTR2QX HTR2QY HTR2QZ HTR2RA HTR2RB HTR2RC HTR2RD HTR2RE HTR2RF HTR2RG HTR2RH HTR2RI HTR2RJ HTR2RK HTR2RL HTR2RM HTR2RN HTR2RO HTR2RP HTR2RQ HTR2RR HTR2RS HTR2RT HTR2RU HTR2RV HTR2RW HTR2RX HTR2RY HTR2RZ HTR2SA HTR2SB HTR2SC HTR2SD HTR2SE HTR2SF HTR2SG HTR2SH HTR2SI HTR2SJ HTR2SK HTR2SL HTR2SM HTR2SN HTR2SO HTR2SP HTR2SQ HTR2SR HTR2SS HTR2ST HTR2SU HTR2SV HTR2SW HTR2SX HTR2SY HTR2SZ HTR2TA HTR2TB HTR2TC HTR2TD HTR2TE HTR2TF HTR2TG HTR2TH HTR2TI HTR2TJ HTR2TK HTR2TL HTR2TM HTR2TN HTR2TO HTR2TP HTR2TQ HTR2TR HTR2TS HTR2TT HTR2TU HTR2TV HTR2TW HTR2TX HTR2TY HTR2TZ HTR2UA HTR2UB HTR2UC HTR2UD HTR2UE HTR2UF HTR2UG HTR2UH HTR2UI HTR2UJ HTR2UK HTR2UL HTR2UM HTR2UN HTR2UO HTR2UP HTR2UQ HTR2UR HTR2US HTR2UT HTR2UU HTR2UV HTR2UW HTR2UX HTR2UY HTR2UZ HTR2VA HTR2VB HTR2VC HTR2VD HTR2VE HTR2VF HTR2VG HTR2VH HTR2VI HTR2VJ HTR2VK HTR2VL HTR2VM HTR2VN HTR2VO HTR2VP HTR2VQ HTR2VR HTR2VS HTR2VT HTR2VU HTR2VV HTR2VW HTR2VX HTR2VY HTR2VZ HTR2WA HTR2WB HTR2WC HTR2WD HTR2WE HTR2WF HTR2WG HTR2WH HTR2WI HTR2WJ HTR2WK HTR2WL HTR2WM HTR2WN HTR2WO HTR2WP HTR2WQ HTR2WR HTR2WS HTR2WT HTR2WU

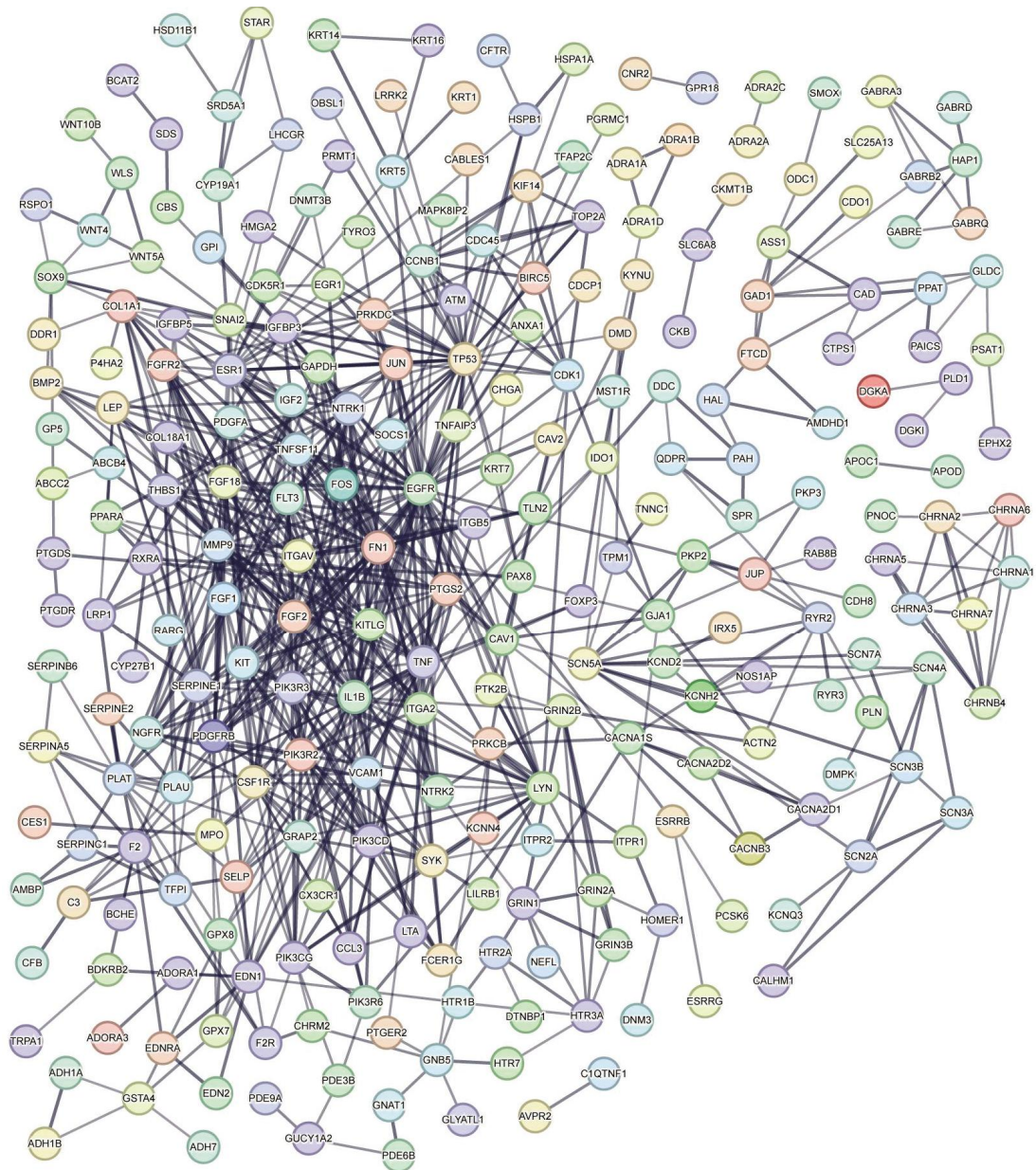


图3 白屈菜治疗 NPC 靶点及其功能相关 PPI 网络图

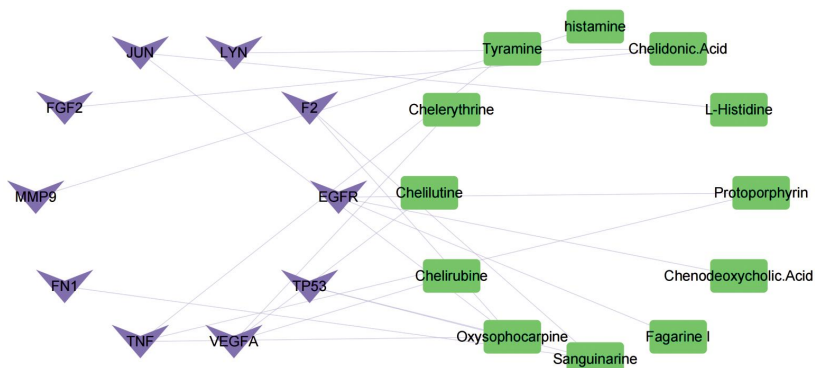


图4 白屈菜抗 NPC 的核心靶点和主要成分

2.6 白屈菜主要活性成分抑制 NPC 细胞增殖

MTT 结果显示,与溶剂对照组比较,顺铂 4 $\mu\text{g}\cdot\text{mL}^{-1}$ 组、不同浓度的血根碱(2.5 $\mu\text{mol}\cdot\text{L}^{-1}$ 、5 $\mu\text{mol}\cdot\text{L}^{-1}$) 组和白屈菜红碱(2.5 $\mu\text{mol}\cdot\text{L}^{-1}$ 、5 $\mu\text{mol}\cdot\text{L}^{-1}$) 组分别作用

于 NPC 5-8F 细胞 24、48 h 后,5-8F 细胞相对增殖率明显降低,差异具有统计学意义($P < 0.01$)。结果见图9。

2.7 白屈菜主要活性成分诱导 NPC 细胞凋亡

与溶剂对照组比较,血根碱 5 $\mu\text{mol}\cdot\text{L}^{-1}$ 组、白

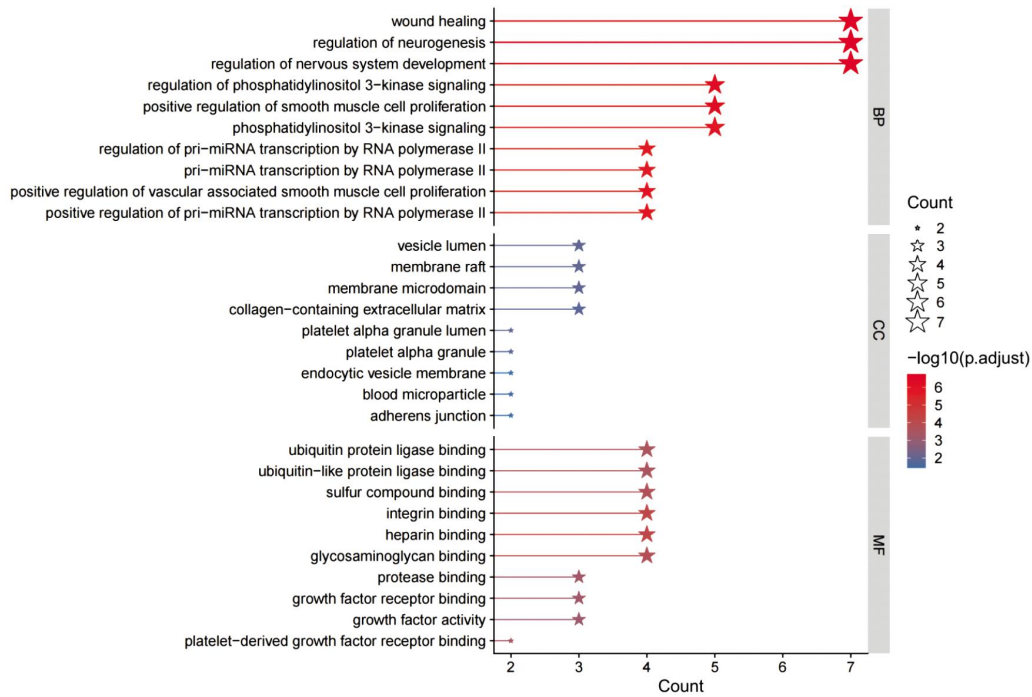


图 5 GO 功能分析星条图

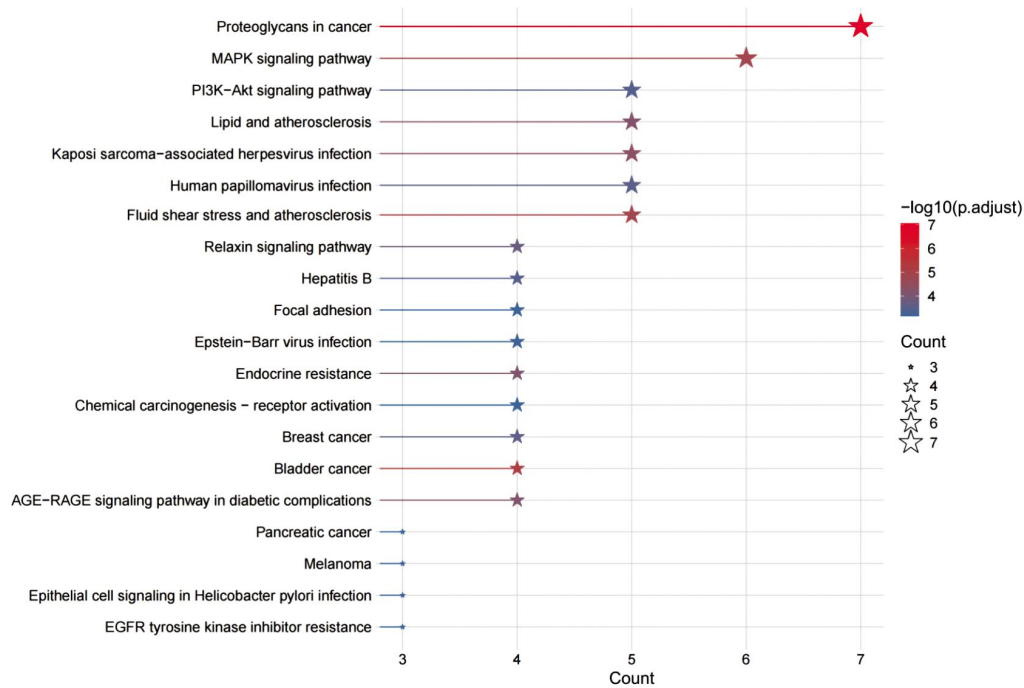


图 6 KEGG 富集分析结果

屈菜红碱 $5 \mu\text{mol}\cdot\text{L}^{-1}$ 组和顺铂 $4 \mu\text{g}\cdot\text{mL}^{-1}$ 组作用于 5-8F 细胞 24 h 后,细胞凋亡率均明显增高,差异具有统计学意义($P<0.01$)。结果见图 10。

2.8 白屈菜主要活性成分对 NPC 细胞增殖和凋亡相关蛋白的影响

Western blot 结果显示,与溶剂对照组比较,血根碱 $5 \mu\text{mol}\cdot\text{L}^{-1}$ 组和白屈菜红碱 $5 \mu\text{mol}\cdot\text{L}^{-1}$ 组的增殖相关蛋白 PCNA 及凋亡相关蛋白 XIAP 的表达水平均降低,差异具有统计学意义($P<0.05$ 或 $P<0.01$); 顺铂 $4 \mu\text{g}\cdot\text{mL}^{-1}$ 组的凋亡相关蛋白 XIAP 的表达水

显著降低,差异具有统计学意义($P<0.01$),增殖相关蛋白 PCNA 的表达水平降低,但差异无统计学意义($P>0.05$)。结果见图 11。

2.9 白屈菜主要活性成分对 NPC 细胞中 AKT、ERK1/2 表达水平的影响

与溶剂对照组比较,血根碱 $5 \mu\text{mol}\cdot\text{L}^{-1}$ 组、白屈菜红碱 $5 \mu\text{mol}\cdot\text{L}^{-1}$ 组、顺铂 $4 \mu\text{g}\cdot\text{mL}^{-1}$ 组中 PI3K/AKT 信号通路关键蛋白 AKT 和 MAPK 信号通路关键蛋白 ERK1/2 的表达水平均显著降低,差异具有统计学意义($P<0.05$ 或 $P<0.01$)。结果见图 12。

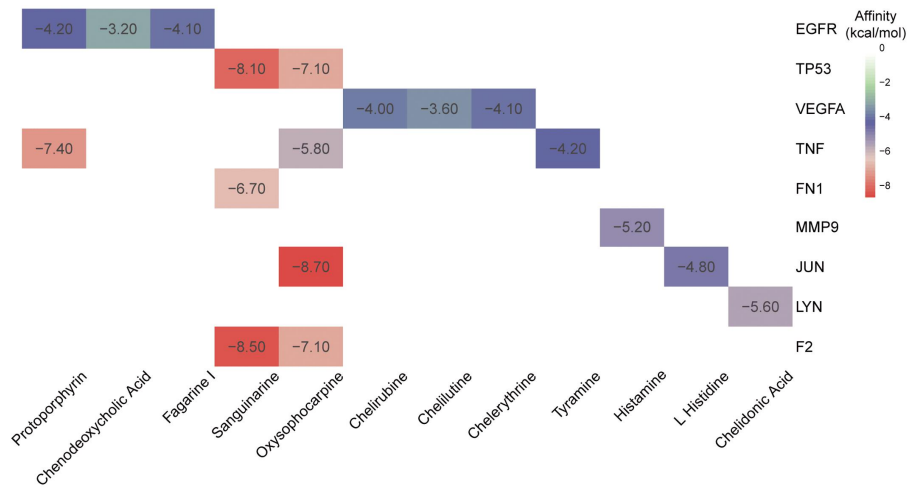


图 7 核心靶点与主要成分的结合能图

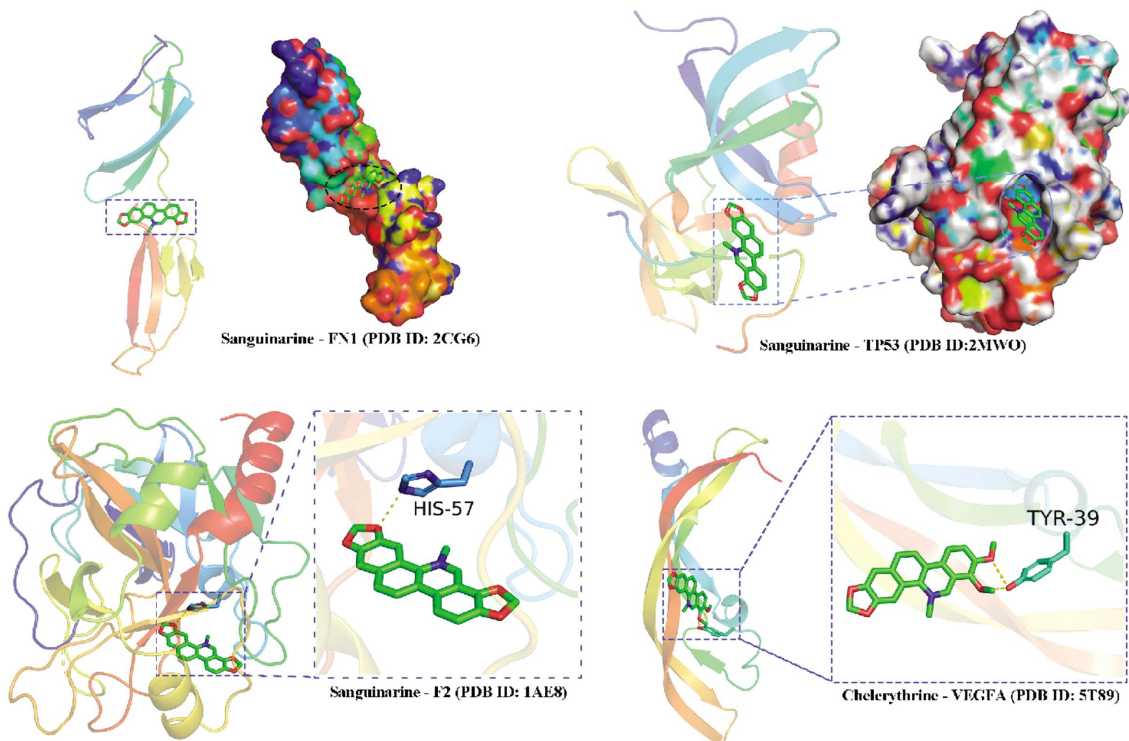


图 8 血根碱、白屈菜红碱与核心靶点的分子对接情况图

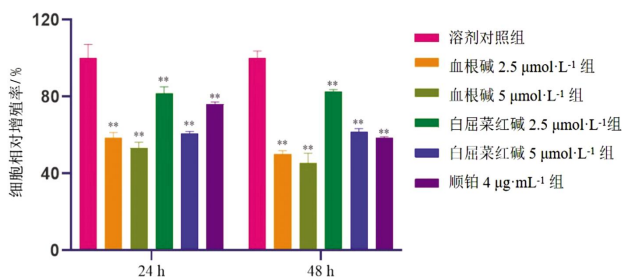


图 9 白屈菜主要活性成分对 5-8F 细胞增殖的影响($n=3, \bar{x} \pm s$)
注:与溶剂对照组相比, ** $P < 0.01$ 。

3 讨论

NPC 是一种上皮源性恶性肿瘤,目前其主要的治疗方法为放化疗。传统的化学药物虽疗效显著,

但毒副作用大、易出现耐药性,如何有效改善,是临床较为关注的问题^[13]。中医学认为,NPC 的主要病机为气虚染毒,治宜益气解毒。白屈菜性凉,味苦,具有较强的抗肿瘤活性,但其治疗 NPC 的物质基础及作用机制尚不明确。

网络药理学通过蛋白质组学、基因组学、生物信息学等数据库检索,从分子和整体水平进行中药的系统分析,获得中药的核心化学成分-蛋白靶点,明确中药的作用机制,为中药研究提供新的思路^[14]。本研究基于网络药理学,挖掘白屈菜治疗 NPC 的物质基础和分子机制。通过数据库筛选,本研究共获得白屈菜的生物活性成分 37 个,并从活性成分-靶点

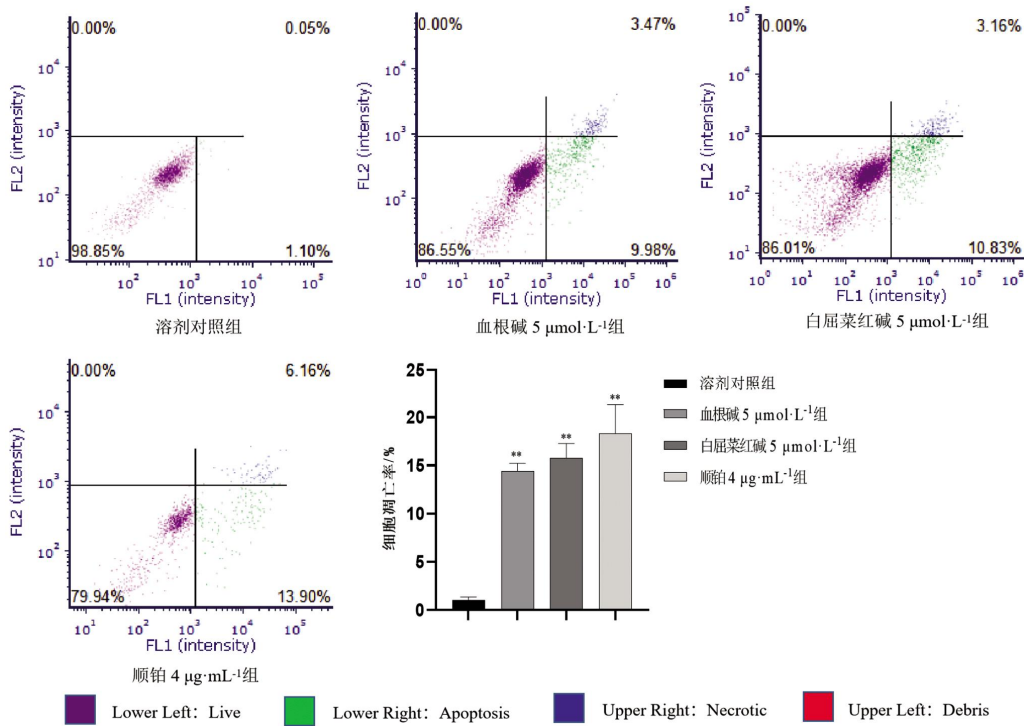


图 10 白屈菜主要活性成分对鼻咽癌 5-8F 细胞凋亡的影响 ($n=3, \bar{x}\pm s$)

注:与溶剂对照组相比, ** $P<0.01$ 。

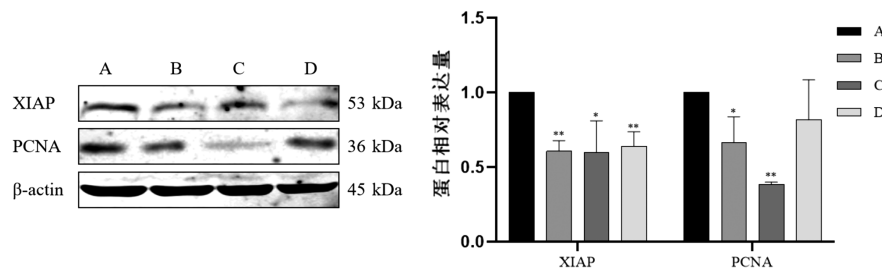


图 11 白屈菜主要成分对 PCNA、XIAP 蛋白表达水平的影响 ($n=3, \bar{x}\pm s$)

注:A.溶剂对照组;B.白屈菜红碱 5 $\mu\text{mol}\cdot\text{L}^{-1}$ 组;C.血根碱 5 $\mu\text{mol}\cdot\text{L}^{-1}$ 组;D.顺铂 4 $\mu\text{g}\cdot\text{mL}^{-1}$ 组。与溶剂对照组相比, * $P<0.05$, ** $P<0.01$ 。

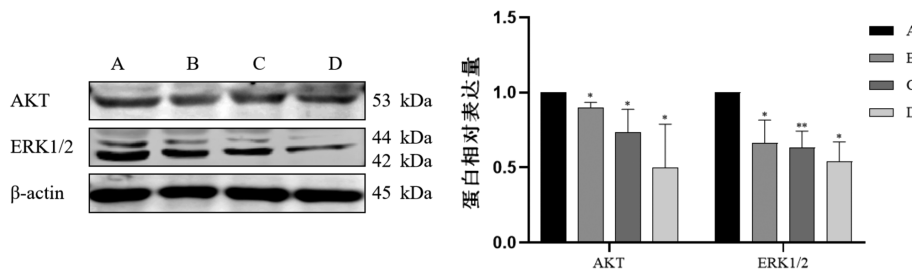


图 12 白屈菜主要成分对 AKT 和 ERK1/2 表达水平的影响 ($n=3, \bar{x}\pm s$)

注:A.溶剂对照组;B.白屈菜红碱 5 $\mu\text{mol}\cdot\text{L}^{-1}$ 组;C.血根碱 5 $\mu\text{mol}\cdot\text{L}^{-1}$ 组;D.顺铂 4 $\mu\text{g}\cdot\text{mL}^{-1}$ 组。与溶剂对照组相比, * $P<0.05$, ** $P<0.01$ 。

相互作用网络构建结果中,得到其关键活性成分血根碱、白屈菜红碱等。研究表明,血根碱可通过影响多细胞靶点、酶的活性及 MAPK、PI3K/AKT 和 NF- κ B 等多个信号传导通路参与肿瘤的发生、发展^[15]。针对 NPC,血根碱能够抑制 NPC 增殖、诱导自噬和凋亡,其作用机制可能与调控 MAPK、PI3K/AKT 和

AMPK/mTOR 信号通路有关^[16-18]。CHMURA 等^[19]通过体外研究证实,白屈菜红碱对 9 种肿瘤细胞均具有抑制作用,且表现出细胞毒性^[20]。这些网络药理学预测结果与近年来研究报道相吻合,说明基于网络药理学的方法预测中药有效成分具有一定的科学性和可行性。同时,本实验证实,血根碱和白屈菜红碱

能够明显抑制 NPC 细胞增殖并诱导细胞凋亡。

通过核心靶点分析得到白屈菜抗 NPC 的核心靶点主要有 EGFR、TP53、VEGFA、TNF、FN1、MMP9、JUN、FGF2、LYN、F2, 主要涉及泛素蛋白连接酶结合、硫化物结合、整合素结合、肝素结合和糖胺聚糖结合等, 并主要富集在 MAPK、PI3K/AKT 等信号通路。MAPK 信号通路的失调和过表达是癌症中最常见的改变, 其主要的家族成员包括 ERK、JNK/SAPK 和 P38MAPK^[21-22]。胡晶等^[23-24]研究发现, 益气解毒方水提物可通过下调 MAPK/ERK 信号通路关键蛋白 p-c-Raf、p-MEK、p-ERK1/2 的表达, 阻滞细胞周期, 抑制 NPC 细胞增殖并诱导细胞凋亡。PI3K/AKT 信号通路在 NPC 生物学进展中发挥了重要作用, 研究表明, 益气解毒方可通过调控 PI3K/AKT 信号通路诱导 NPC 细胞自噬并促进凋亡^[25-26]。在本文 Western blot 实验中, 证实白屈菜相关活性成分白屈菜红碱、血根碱使 NPC 凋亡相关蛋白 XIAP、增殖相关蛋白 PCNA、MAPK 信号通路相关蛋白 ERK1/2、PI3K/AKT 通路相关蛋白 AKT 下调, 佐证了网络药理学对白屈菜活性成分及相关通路靶点网络的有效性。

综上所述, 本研究系统预测了白屈菜治疗 NPC 的作用机制, 且证实了血根碱、白屈菜红碱是白屈菜抗 NPC 的重要物质基础, MAPK、PI3K/AKT 信号通路可能是其发挥抗 NPC 作用的重要机制, 为白屈菜临床干预 NPC 提供了一定的理论依据。

参考文献

- [1] 何文龙, 吕炎, 胡云扬, 等. 放射联合药物治疗鼻咽癌的现状[J]. 实用癌症杂志, 2019, 34(2): 3.
- [2] PETERSSON F. Nasopharyngeal carcinoma: A review[J]. *Seminars in Diagnostic Pathology*, 2015, 32(1): 54-73.
- [3] 邱元正, 刘超, 李果. 鼻咽癌放射治疗的现状与对策[J]. 中国耳鼻咽喉颅底外科杂志, 2015, 21(6): 435-438.
- [4] 黄自丽, 黄修燕, 郑起. 中药抗肿瘤作用及其作用机制研究进展[J]. 医学综述, 2010, 16(3): 386-389.
- [5] 山尔. 《救荒本草》校释与研究出版[J]. 中华医史杂志, 2007, 37(2): 1.
- [6] 洪波, 孟琦, 江健梅, 等. 白屈菜生物碱研究进展[J]. 人参研究, 2022, 34(2): 58-62.
- [7] 赵国成, 张国财. 白屈菜人工栽培及加工处理技术的研究[J]. 中国林副特产, 2022, 180(5): 22-24.
- [8] 李学哲, 朴惠顺. 异喹啉类生物碱的抗肿瘤作用及机制的研究进展[J]. 华西药理学杂志, 2014, 29(1): 94-97.
- [9] 宗永立, 刘艳平. 白屈菜红碱对人胃癌 BGC823 细胞的增殖抑制和凋亡诱导作用[J]. 中草药, 2006, 37(7): 1054-1056.
- [10] 邹翔, 王雨蒙, 王嘉琪, 等. 白屈菜碱的药理作用研究进展[J]. 现代药物与临床, 2014, 29(11): 1326-1330.
- [11] 何苗. 白屈菜红碱联合厄洛替尼抗非小细胞肺癌的作用机理研究[D]. 长春: 吉林大学, 2017.
- [12] YANG T, XU R, SU Q, et al. Chelerythrine hydrochloride inhibits proliferation and induces mitochondrial apoptosis in cervical cancer cells via PI3K/BAD signaling pathway[J]. *Toxicology in Vitro*, 2020, 68: 104965-104965.
- [13] 谢民强. 鼻咽癌治疗研究进展[J]. 中国耳鼻咽喉颅底外科杂志, 2023, 29(6): 1-10.
- [14] 刘鑫旭, 吴嘉瑞, 张丹, 等. 基于网络药理学的参附汤作用机制分析[J]. 中国实验方剂学杂志, 2017, 23(16): 211-218.
- [15] DING Z H, TANG S C, WEERASINGHE P, et al. The alkaloid sanguinarine is effective against multidrug resistance in human cervical cells via bimodal cell death[J]. *Biochemical Pharmacology*, 2002, 63(8): 1415-1421.
- [16] 彭佳欣, 陶阳阳, 彭江敏, 等. 血根碱联用 5-氟尿嘧啶对鼻咽癌裸鼠移植瘤细胞自噬和凋亡的影响[J]. 中国药理学杂志, 2022, 57(24): 2092-2098.
- [17] 苏俐丹, 何迎春, 黄立中, 等. AMPK/mTOR 信号通路介导的自噬在血根碱抑制鼻咽癌细胞增殖中的作用研究[J]. 中国免疫学杂志, 2022, 38(23): 2870-2875.
- [18] 谭爱军. 血根碱通过 MAPK/ERK 信号通路抑制鼻咽癌细胞增殖的研究[D]. 长沙: 湖南中医药大学, 2021.
- [19] CHMURA S J, DOLAN M E, CHA A, et al. In vitro and in vivo activity of protein kinase C inhibitor chelerythrine chloride induces tumor cell toxicity and growth delay in vivo[J]. *Clinical Cancer Research*, 2000, 6(2): 737-742.
- [20] 罗飞亚, 马新群, 林飞. 白屈菜红碱对大鼠的长期毒性试验研究[J]. 癌变·畸变·突变, 2014, 26(6): 459-462.
- [21] GORRINI C, HARRIS I S, MAK T W. Modulation of oxidative stress as an anticancer strategy[J]. *Nature Reviews Drug Discovery*, 2013, 12: 931-947.
- [22] 范慧宁, 张靖, 朱金水. 血根碱抗肿瘤机制的研究进展[J]. 现代肿瘤医学, 2019, 27(18): 3323-3327.
- [23] 胡晶, 戴娜, 徐冰雁, 等. 益气解毒方通过 MAPK/ERK 信号通路抑制鼻咽癌细胞增殖[J]. 中国中药杂志, 2018, 43(6): 1221-1227.
- [24] 胡晶, 刘洁, 徐冰雁, 等. MAPK/ERK 信号通路在益气解毒方水提物诱导鼻咽癌细胞凋亡中的作用[J]. 中国药理学通报, 2019, 35(11): 1613-1621.
- [25] 蔺婷, 戴娜, 罗晶婧, 等. 益气解毒方通过 PI3K/AKT/mTOR 信号通路诱导鼻咽癌细胞自噬的研究[J]. 中华中医药杂志, 2020, 35(3): 1484-1488.
- [26] 蔺婷, 罗晶婧, 周芳亮, 等. 益气解毒方通过诱导自噬促进鼻咽癌细胞凋亡的作用研究[J]. 中药新药与临床药理, 2019, 30(10): 1149-1158.

(本文编辑 贺慧斌)